A Two-Joint Human Posture Control Model With Realistic Neural Delays

Yao Li, *Member, IEEE*, William S. Levine, *Fellow, IEEE*, and Gerald E. Loeb, *Senior Member, IEEE*

***Abstract*—During quiet standing, humans tend to sway with a distinctive pattern that has been difficult to capture with simple engineering models. We have developed a nonlinear optimal control model for posture regulation. The proposed model consists of two main components: body dynamics and performance measure. The body dynamics are those of a double inverted pendulum in the sagittal plane controlled by ankle and hip torques. The performance measure is nonlinear quartic in the center of pressure and quadratic in the controls. Realistic values for both sensory and motor delays are included in the dynamic model. This nonlinear quartic regulator problem is solved approximately by the model predictive control technique. The resulting feedback control replicates both the experimentally observed sway and the coordinated nonlinear response. It should also use less muscular energy than other comparable controls. The method can easily be extended to more complex models of posture regulation.**

***Index Terms*—Convex optimization, model predictive control (MPC), neural delay, nonlinear optimal control, postural sway.**

I. Introduction

BALANCE control during quiet standing involves the central nervous system (CNS), the musculoskeletal system and the sensorimotor processes. The controller must integrate real time sensory data coming from the vestibular system, joint angle proprioceptors, tactile force sensors, and visual perception [1]. Control performance can be degraded by various physiological conditions, including aging [2], [3]; disruption or alteration of proprioception [4]–[7]; disruption or obstruction of vision [2], [8], [9] and alteration of vestibular transduction [4], [10]–[12]. As with any motor skill, postural balance control can improve with training [13]. One remarkable feature of human postural regulation is the existence of small amplitude, spontaneous back-and-forth sway in the sagittal plane. The quantitative and qualitative properties of the constant sway phenomenon have been extensively investigated. Early studies used the direct measurement of the trajectory of the ankle joint angle [6], [7], [14], the center of mass (COM) [3], [15], [16], the center of pressure (COP) [8], [15], [17], and other body points [1], [18] as measures of the extent of the sway. The effects from, and on, all relevant sensory modalities have also been studied qualitatively and quantitatively, including proprioceptive [4], [11], vestibular [10], visual [1], [3], [19] and somatosensory [6], [20], [21].

This work is based on the following reasoning. Any smooth (i.e., differentiable) dynamical system must be approximately linear for small inputs or perturbations. Because the human posture regulation system is smooth, the controller must be approximately linear for small perturbations. Thus, one possible explanation for the observed sway is that the feedback controller is nonlinear with a slope of zero at the equilibrium point. The linear quadratic regulator (LQR) has been proposed by several researchers as a model for posture control [22], [23]. However, the solution is always a linear feedback control that never has zero gain at the equilibrium point. Changing the performance measure to one that is quartic (or higher even order) in the states and quadratic in the controls results in an optimal controller that is nonlinear with zero slope at equilibrium. This paper tests the hypothesis that a model system employing such an optimal controller matches the experimentally observed sway behavior.

We first review prior literature on optimal control of posture and movement and introduce model predictive control (MPC) [24]–[26]. This is followed by a derivation of a mechanical model of the quietly standing human to which we add various estimates of delays in the sensorimotor system. We then test the hypothesis that the postural control system is trying to minimize a performance measure that is quartic in the COP and quadratic in the controls. The resulting optimal control problem cannot be solved analytically so an approximate feedback solution is established using MPC techniques. This method is believed to be of widespread applicability to biomechanical control problems. The solution to the optimal control problem is shown to exhibit the above-mentioned characteristics of sway in quietly standing humans, including different coordinated responses to different size perturbations. These solutions would use substantially less energy than the comparable LQR. The paper concludes with a description of several specific important and straightforward ways in which this research can be extended.

II. Background

There has been an intensive effort to identify and model the underlying mechanisms of human postural control [1], [22], [27]–[29]. Such a model could be useful for clinical tests on humans as they perform balance tasks, could aid in the clinical diagnosis and treatment of motor control disorders, and could contribute to the development of prostheses, including functional electrical stimulation for recovery of lost motor function [2], [30].

Manuscript received November 08, 2011; revised March 15, 2012; accepted April 18, 2012. Date of publication June 06, 2012; date of current version September 07, 2012. This work was supported in part by the DARPA REPAIR program.

Y. Li and G. E. Loeb are with the Department of Biomedical Engineering, University of Southern California, Los Angeles, CA 90089 USA (e-mail: yao.li.1@usc.edu; gloeb@usc.edu).

W. S. Levine is with the Department of Electrical and Computer Engineering, University of Maryland, College Park, MD 20740 USA (e-mail: wsl@umd.edu).

Digital Object Identifier 10.1109/TNSRE.2012.2199333

Optimal controls have been proposed as models of a variety of motor tasks [31], [32]. For example, a unified theory of eye and arm movements based on the idea that the controller minimized the variance of position was proposed by Harris and Wolpert [50]. Their theoretical predictions provided a good match to their experimental observations. Another example is the comparison of static and dynamic optimization techniques for computing the muscle forces used by humans as they walk [51]. One of the issues in the application of optimal control to motor control is the choice of performance measure. One useful approach is to specify a task that, in itself, involves optimization. Two examples are jumping as high as possible [52] and pedaling a bicycle as fast as possible [53].

There have been a number of attempts to understand the regulation of posture by means of an optimal control model. Kuo proposed a triple linked inverted pendulum model and a linear quadratic Gaussian (LQG) optimal controller as a model of balance regulation [22]. The LQG controller consisted of a LQR controller and a linear quadratic estimator (LQE) for state feedback information [33]. In Kuo's model, muscle dynamics were not included, joint torques were directly proportional to motor output of the controller and neural delays were mentioned but not quantified. While there is no evidence that the CNS actually functions as an LQG controller, this is one plausible way to achieve realistic performance goals with redundant sets of both actuators and sensors. He, Levine and Loeb [23] developed a model of the neuromusculoskeletal system of the standing cat that included an LQR optimal controller. They used this model to compute and compare control solutions that minimized various cost functions representing deviations in joint positions, muscle lengths, and muscle stiffness. Johansson *et al.* [34] proposed a similar model for posture and movement.

There are two major difficulties in applying optimal control theory to problems in neurophysiology and in engineering. First, it is extremely difficult to find *optimal feedback* controls. In order to do so, one has to solve the *Hamilton Jacobi Bellman Caratheodory* (HJBC) partial differential equation. Only a handful of problems have been solved; most of them are trivial. The LQG optimal control problem is the very important and useful exception and that is why it has been applied so extensively in these early studies. Second, a computational solution to the HJBC partial differential equation is also impossible except for a small number of problems. Over the last 30 years, control engineers have developed a methodology, model predictive control (MPC) or receding horizon control (RHC), to find approximately optimal feedback solutions to otherwise intractable control problems. The MPC method is based on an iterative approach in discrete time, which provides a way to convert a sequence of open-loop optimal controls to an approximately optimal closed-loop control. It has by now been used in thousands of practical applications [35].

The cornerstone of MPC is the repeated solution of a sequence of open-loop optimal control problems. The first step in MPC is to approximate the original continuous-time problem by a discrete-time one. Once one discretizes the time, open-loop optimal control problems with known initial conditions become nonlinear programming problems, which can then be solved quickly, efficiently, and accurately. Specifically, at the initial time, the optimal control is computed as a function of the state vector at $t = 0$, $x(0)$, which is assumed known in the theory. In practice, an estimate of $x(0)$ based on all the data available prior to $t = 0$ is used. The computed control is then applied on the interval, $0 \leq t \leq \delta$, where δ is the sampling interval. At $t = \delta$ a new optimal open-loop control is calculated based on the new initial state—the state vector at $t = \delta$. This assumes the computation can be done instantaneously, which is not possible. In practice, the best available estimate of the state at $t = \delta$ based on the data available at $t = 0$ is used. This gives an interval of duration δ to do the computations. The new open-loop optimal control is then applied to the system during the interval $\delta \leq t \leq 2\delta$. This idea is illustrated in Fig. 1. This iterative procedure then continues indefinitely using the state estimate of the initial condition at time $t = k\delta$ as the initial condition for computing the control that is applied during $k\delta \leq t \leq (k+1)\delta$. The state estimate is a prediction of the state $x(k\delta)$ using the data available at $t = (k-1)\delta$.

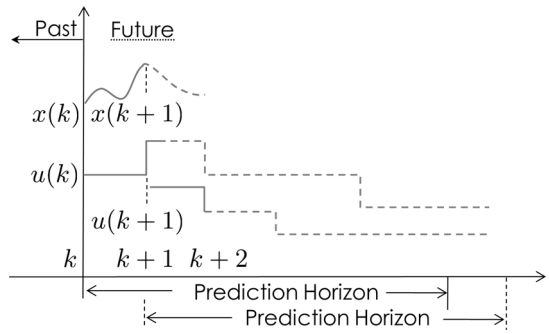

Fig. 1. MPC model. At time k, optimal control $u(i), k \leq i \leq k+N-1$ is computed using the true initial condition $x(k)$. First control value $u(k)$ is applied. Then, at time $(k+1)$, a new optimal control $u(i), k+1 \leq i \leq k+N$ is computed using true initial condition $x(k+1)$ and control value $u(k+1)$ is applied. This procedure—compute optimal control over a prediction horizon of duration N but apply only the first value—is then repeated indefinitely. Note that procedure produces a closed-loop control because applied control value always depends on current state.

III. Mathematical Model

A. Mechanical System

The human body exhibits redundant multiple degree-of-freedom (DOF) motion. Normally, only the most relevant body segments and joints are considered for the balance control problem. These segments of interest are the feet, legs, thighs, trunk, and head, while the corresponding joints are the ankle, knee, hip, and neck. Depending on the level of detail desired, some segments may be lumped.

In the study of upright posture, the human is commonly modeled as a single inverted pendulum in which all body segments above the ankles are lumped to form one rigid body and the feet are considered as the supporting surface [12], [30], [36], [37]. Experimental observations show that the response to perturbations during quiet standing varies both quantitatively and qualitatively with different sizes of the disturbance. For small perturbations, the response involves primarily motion at the ankle with other joint angles held approximately constant, while larger

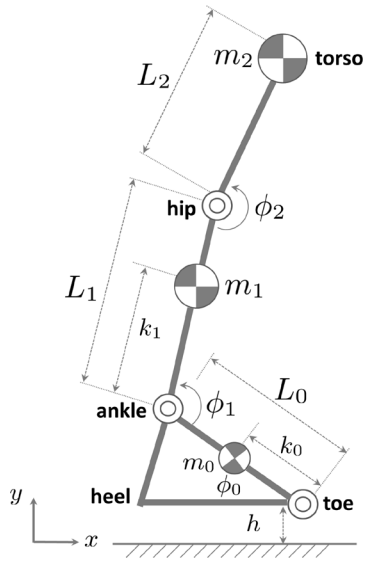

Fig. 2. Three link sagittal biped is composed of three rigid links. Term k_i for $i = 0, 1, 2$ is distance from the bottom of link i to center of mass of link i. Term L_i is length of link i.

perturbations generate substantial motion at both ankle and hip joints. In order to account for the full range of perturbations and responses, our computational model consists of three rigid connected segments to represent the foot, leg (locked knee), and torso as depicted in Fig. 2.

This is consistent with considerable experimental data that indicate that humans keep their knee angle nearly constant for a range of sizes of perturbations to their posture.

For very large perturbations they will bend their knees. Still larger perturbations often require a step to prevent falling. We first derived the equations of motion using the Euler-Lagrange method for this two joint, three segment model controlled by torques on the ankle and hip joints

$$\frac{d}{dt}\left(\frac{\partial \mathcal{L}}{\partial \dot{\phi}_1}\right) - \frac{\partial \mathcal{L}}{\partial \phi_1} = u_a \tag{1}$$

$$\frac{d}{dt}\left(\frac{\partial \mathcal{L}}{\partial \dot{\phi}_2}\right) - \frac{\partial \mathcal{L}}{\partial \phi_2} = u_h \tag{2}$$

$$\mathcal{L} = \mathcal{K} - \mathcal{P} \tag{3}$$

and $\mathcal{K}$ is the total kinetic energy and $\mathcal{P}$ is the total potential energy of the dynamic system. We then used a method [55] to determine the forces of constraint that act on the foot. These forces are needed because they determine the location of the COP. The method is to introduce a degree of freedom for each constraint. The resulting Euler-Lagrange equations can then be solved for the generalized forces of constraint. We introduced two extra degrees of freedom: the toe angle ϕ_0 and the vertical displacement of the toe h, to enable us to compute the location of the COP l_{cop}. The control torque at the toe and the ground reaction force are

$$u_t = \frac{d}{dt}\left(\frac{\partial \mathcal{L}}{\partial \dot{\phi}_0}\right) - \frac{\partial \mathcal{L}}{\partial \phi_0} \tag{4}$$

$$f_v = \frac{d}{dt}\left(\frac{\partial \mathcal{L}}{\partial \dot{h}}\right) - \frac{\partial \mathcal{L}}{\partial h} \tag{5}$$

Thus, the generalized coordinates for the overall system are $[\phi_0, \phi_1, \phi_2, h]$, where ϕ_1 is the ankle angle and ϕ_2 is the hip angle. The torques at the toe, ankle and hip joint are u_t, u_a and u_h. The term f_v is the vertical component of the ground reaction force. The horizontal component of the ground reaction force can be ignored because the foot does not move and the horizontal force exerts no torque about the toe. The total kinetic energy is the sum of the rotational and translational kinetic energies of the components of the system, while the potential energy is all due to gravity. Both kinetic and potential energies were then written in terms of the four generalized coordinates and their first derivatives. These were then used to write the four Euler-Lagrange equations (1), (2), (4), and (5). We then set $h = 0$ and $\phi_0 = \text{constant}$ as constraints. This makes all the derivatives zero, i.e., $\dot{\phi}_0 = \ddot{\phi}_0 = 0$ and $h = \dot{h} = \ddot{h} = 0$. At this point the first two Euler-Lagrange equations (1) and (2) are unchanged from their original form and give the body dynamics of the system. The resulting complete expressions for the body dynamics with ankle and hip torque are

$$\begin{bmatrix} Q_{11} & Q_{12} \\ Q_{21} & Q_{22} \end{bmatrix} \begin{bmatrix} \ddot{\phi}_1 \\ \ddot{\phi}_2 \end{bmatrix} + \begin{bmatrix} R_1 \\ R_2 \end{bmatrix} = \begin{bmatrix} u_a \\ u_h \end{bmatrix} \tag{6}$$

$$\begin{aligned} Q_{11} &= I_1 + m_1 k_1^2 + m_2 L_1^2 + m_2 L_2^2 \\ &\quad + m_2 L_1^2 + 2 m_2 L_1 k_2 \\ Q_{12} &= Q_{21} = m_2 k_2^2 + m_2 L_1 k_2 \\ Q_{22} &= I_2 + m_2 k_2^2. \end{aligned}$$

$$\begin{aligned} R_1 &= (m_1 k_1 + m_2 L_1)(\cos\phi_0 \cos\phi_1 + \sin\phi_0 \sin\phi_1) g \\ &\quad - m_2 k_2 [\cos\phi_0 \cos(\phi_2 + \phi_1) + \sin\phi_1 \sin(\phi_2 + \phi_1)] g \\ R_2 &= -m_2 k_2 \cos(\phi_2 + \phi_1 - \phi_0) g. \end{aligned}$$

Experimentally, the COP is estimated from the weighted average of pressure distributed over the contact surface area of the force platform. The COP is precisely defined by the torque at the toe u_t and the ground force vector acting on the foot f_v. The toe torque can be eliminated by applying the ground force at the distance from the toe that creates u_t. This distance is the location of the COP, mathematically denoted by l_{cop} (f_v is orthogonal to l_{cop})

$$l_{\text{cop}} = \frac{u_t}{f_v}. \tag{7}$$

The control torque at the toe and the ground reaction force are precisely written as follows:

$$\begin{aligned} u_t &= \left[-\left(m_1 k_1^2 + m_2 L_1^2 + m_2 k_2^2\right) + 2 m_2 L_1 k_2 \cos\phi_2 \right. \\ &\quad + (m_1 L_0 k_1 + m_2 L_0 L_1) \cos\phi_0 \cos(\phi_1 - \phi_0) \\ &\quad \left. - m_2 L_0 k_2 \cos\phi_0 \cos(\phi_2 + \phi_1 - \phi_0) \right] \ddot{\phi}_1 \\ &\quad + \left[-m_2 k_2^2 + m_2 L_1 k_2 \cos\phi_2 \right. \\ &\quad \left. - m_2 L_0 k_2 \cos\phi_0 \cos(\phi_2 + \phi_1 - \phi_0) \right] \ddot{\phi}_2 \\ f_v &= (m_1 k_1 + m_2 L_1) \cos(\phi_1 - \phi_0) \ddot{\phi}_1 \\ &\quad - (m_2 k_2 + m_2 L_2) \cos(\phi_2 + \phi_1 \\ &\quad - \phi_0)(\ddot{\phi}_2 + \ddot{\phi}_1) + Mg. \end{aligned}$$

TABLE I
BODY SEGMENT LENGTH AND WEIGHT EXPRESSED AS FRACTION OF ENTIRE BODY

Foot	**Shank**	**Torso**
$m_0 = \frac{2}{35}M$	$m_1 = \frac{6}{35}M$	$m_2 = \frac{27}{35}M$
$k_0 = 0.094L$	$k_1 = 0.28L$	$k_2 = 0.436L$
$L_0 = 0.117L$	$L_1 = 0.464L$	$L_2 = 0.436L$

B. Equilibrium Posture

We first linearize the multi-segment inverted pendulum model around an unstable vertical equilibrium point $\underline{p}^*$ by $\underline{p} = \underline{p}^* + \Delta\underline{p}$, where $\Delta\underline{p}$ is a small deviation from $\underline{p}^*$. Here, $\phi_1^* = \pi/2 + \phi_0$, $\phi_2^* = \pi$ and all the other nominal values are zero. Because the perturbations of the upright posture that are being considered are small, it is reasonable to linearize about this defined nominal vertical posture

$$\underline{p} = \begin{pmatrix} \phi_1^* \\ \phi_2^* \\ \dot{\phi}_1^* \\ \dot{\phi}_2^* \\ u_a^* \\ u_h^* \end{pmatrix} + \begin{pmatrix} \Delta\phi_1 \\ \Delta\phi_2 \\ \Delta\dot{\phi}_1 \\ \Delta\dot{\phi}_2 \\ \Delta u_a \\ \Delta u_h \end{pmatrix}. \tag{8}$$

By introducing the state variables $\underline{x}$ and the control vector $\underline{u}$

$$\underline{x} = \begin{bmatrix} x_1 \\ x_2 \\ x_3 \\ x_4 \end{bmatrix} = \begin{bmatrix} \Delta\phi_1 \\ \Delta\phi_2 \\ \frac{d\Delta\phi_1}{dt} \\ \frac{d\Delta\phi_2}{dt} \end{bmatrix} \quad \underline{u} = \begin{bmatrix} u_1 \\ u_2 \end{bmatrix} = \begin{bmatrix} \Delta u_a \\ \Delta u_h \end{bmatrix}$$

we convert the dynamics into

$$\dot{\underline{x}} = A\underline{x} + B\underline{u}. \tag{9}$$

Morphometric parameters tend to differ among subjects, making it difficult to understand the relationship between human performance and idealized models. Therefore, we introduce the normalization factor $\beta = \sqrt{L/g}$, which has dimension $[\beta] = T$ (time). Then a dimensionless "time" is defined as $\tau = t/\beta$, the derivative is $d\tau/dt = 1/\beta$. Now we have $\phi_i(\tau) = \phi_i(t/\beta)$, for $i = 0, 1, 2$. For simplicity, we use ϕ_i to denote $\phi_i(\tau)$ in the rest of the paper. We choose $\boldsymbol{M}$ to be the total body mass and $\boldsymbol{L}$ to be the height of the upright body and each segment is proportional to these two quantities. In reality, the fractions would have to be measured or estimated for a specific individual, here we use the typical numerical values as listed in Table I [38].

Now, we have a completely dimensionless system defined as

$$\dot{\underline{x}}(t) = A\underline{x}(t) + B\underline{u}(t) \tag{10}$$

$$\underline{x}(t) = \begin{bmatrix} \phi_1(t) \\ \phi_2(t) \\ \dot{\phi}_1(t) \\ \dot{\phi}_2(t) \end{bmatrix} \quad \underline{u}(t) = \begin{bmatrix} u_1(t) \\ u_2(t) \end{bmatrix} \tag{11}$$

where

$$A = \begin{bmatrix} 0_{2\times 2} & I_{2\times 2} \\ \beta^2 \left(\frac{\mathrm{Q}}{ML^2}\right)^{-1} \frac{\mathrm{R}}{ML^2} & O_{2\times 2} \end{bmatrix}$$

$$B = \begin{bmatrix} O_{2\times 2} \\ \beta^2 \left(\frac{\mathrm{Q}}{ML^2}\right)^{-1} \frac{1}{ML^2} \end{bmatrix}. \tag{12}$$

The COP is a function of all the states and controls

$$l_{\mathrm{cop}}(\underline{p}) = f(\phi_1, \phi_2, \dot{\phi}_1, \dot{\phi}_2, u_1, u_2). \tag{13}$$

For small perturbations, we can also linearize l_{cop} about the nominal state $\underline{p}^*$, and the linear approximation Δl_{cop} is

$$\Delta l_{\mathrm{cop}}(\underline{p}) = \nabla l_{\mathrm{cop}}(\underline{p}^*)\Delta\underline{p} \tag{14}$$

where

$$\nabla l_{\mathrm{cop}}(\underline{p}^*) = \left[\left.\frac{\partial l_{\mathrm{cop}}}{\partial \phi_1}\right|_{\underline{p}^*} \quad \left.\frac{\partial l_{\mathrm{cop}}}{\partial \phi_2}\right|_{\underline{p}^*}, \quad \cdots, \quad \left.\frac{\partial l_{\mathrm{cop}}}{\partial u_h}\right|_{\underline{p}^*} \right]. \tag{15}$$

C. Delay

Neural delay has been shown to play a significant role in the balance control system for quiet stance [39], [40]. Neural delay can be defined as the total time interval between the presentation of a stimulus and the evocation of a response. It depends on the length of the neural path between the receptor organ and the responding muscles, the time that the CNS requires to process the information, and the time it takes for a muscle to develop force once it is excited. Myers [41] decomposes the neural delay in the human motor control system into four sequential components: sensation, perception, conduction and execution.

Sway can be detected by proprioception (e.g., stretch of ankle muscles), vestibular function (i.e., translational acceleration of the semicircular canals in the head), and vision (e.g., optical flow from relative motion of surrounding objects). Proprioceptive reflexes through the spinal cord require the least time. If the muscles are not slack, changes in joint angle cause essentially instantaneous changes in muscle length that are transduced by muscle spindle primary afferents essentially instantaneously. Their sensory axons conduct at the fastest velocity in the body ($\sim$80 m/s in humans) over the $\sim$1 m distance from receptors in calf muscles to lumbar spinal cord, representing a sensation delay of $\sim$12.5 ms. They make monosynaptic connections to the motoneurons that innervate the calf muscles, representing a "perception" delay as short as $\sim$1 ms depending on the strength of the signals. The axons of the motoneurons also conduct at about 80 m/s for the return trip of 1 m, producing a conduction delay of $\sim$12.5 ms plus $\sim$1 ms for synaptic transmission to muscle fibers. This means that monosynaptic reflex reactions can be initiated in as little as 25 ms [54], [56] but posture regulation also involves other sensors and longer neural pathways.

Visual and vestibular stimuli require more signal processing and must be transmitted over longer distances from the head. Weak stimuli can result in substantially longer delays through multiple synapses. Visual sensation is slowed by temporal integration in the photoreceptors and retinal circuitry, which can add $\sim$100 ms depending on light levels. Voluntary responses require considerable cortical processing for perception, so they generally have a latency of $\sim$200–300 ms, depending on the nature of the sensory cue [42]. In addition to the delays in transduction and transmission, there is an activation delay in the muscles themselves, which can be modeled most accurately as a dynamic lag but approximating it by a delay of 50–80 ms is reasonably accurate. Therefore, we included 100, 200, and 300 ms delays in these simulations to bracket the range of delays occurring in

the neural control of sway. The larger the delay, the more difficult it is to find appropriate control gains to stabilize the system.

It is still unclear how the CNS evokes a timely active torque despite a long time delay in the sensorimotor feedback control loop. In control engineering, if delays are long and external conditions change rapidly, specific feedback corrections may not be appropriate by the time they are implemented. In order to model the neural delay in the MPC-based nonlinear optimal control model, we introduce two distinct variables to account for the four different delay stages: τ_s is the lumped delay of sensation and perception, which gives us a vector of delayed observations, $\underline{y}(t) = \underline{x}(t-\tau_s)$; and τ_a is the lumped delay of transduction and execution, which gives us a vector of delayed control $\underline{u}(t-\tau_a)$. We include these in the biomechanical model as

$$\dot{\underline{x}}(t) = A\underline{x}(t) + B\underline{u}(t-\tau_a). \tag{16}$$

In reality there is likely to be a slightly shorter delay in signals to the hip muscles than to the ankle muscles. This could be roughly 25 ms so it is not likely to have a large effect on our results. It would be interesting to investigate this in the future.

Another future investigation would be to model the accuracy, errors, and delays in vision, proprioception, and the sensing of accelerations. This would enable us to study the contribution of the different sensory modalities to postural sway, and the effect of removing one or more sensory modalities on the maintenance of posture.

D. Performance Measure

We hypothesize a nonlinear optimal control model in which the performance measure is nonlinear quartic (NQ) or higher even order in the states. i.e.,

$$J = \frac{1}{2}\int_0^\infty \left[q l_{\text{cop}}^4(t) + r_1 u_1^2(t) + r_2 u_2^2(t)\right] dt \ (*)$$

where q, r_1 and r_2 are cost coefficients, and l_{cop} is deviation from the nominal equilibrium value of the COP in the sagittal plane (x coordinate) [43]–[45]. The variables u_1 and u_2 are the deviations from the equilibrium values of the controls. The COP is a good indicator of stability, and the human body has the sensors necessary to provide the CNS with good estimates of the COP. The optimal control problem is to find $u(t)$ for all $0 \le t < \infty$ so as to minimize performance measure$(*)$, subject to $\dot{\underline{x}}(t) = A\underline{x}(t) + B\underline{u}(t-\tau_a)$ and $\underline{y}(t) = \underline{x}(t-\tau_s)$.

E. Noise and Perturbations

There is a small amount of noise inherent in muscle activation and neural sensing. The standard experiments on posture regulation deliberately introduce additional perturbations to the nominal posture, so the noise is essential to the sway. We model both intrinsic noise and perturbations as white Gaussian noise (WGN). To avoid the difficulties of writing a stochastic differential equation in a mathematically precise form, we include the noise and random perturbations in the discrete-time approximation where the notational problems do not exist [see (21) and (22)].

IV. Solution

Because the continuous-time, infinite duration, optimal control problem described in the previous paragraph does not have an analytical solution, an approximately optimal feedback solution can be found by the MPC method. The first step is to define a sampling interval δ so that $\tau_a = n_a\delta$, and we use $t = k\delta$ to transform the continuous state-space system into a discrete-time system. To determine the coefficient matrices of the discrete-time system, we use (17) and (18) to analyze the $(k+1)$ term

$$\underline{x}(k) = e^{Ak\delta}\underline{x}(0) + \int_0^{k\delta} e^{A(k\delta-\xi)}Bu(\xi)d\xi \tag{17}$$

$$x(k+1) = e^{A(k+1)\delta}\underline{x}(0) + \int_0^{(k+1)\delta} e^{A((k+1)\delta-\xi)}Bu(\xi)d\xi \tag{18}$$

$$x(k+1) = e^{A\delta}[e^{kA\delta}\underline{x}(0)] + e^{A\delta}\int_0^{k\delta} e^{A(k\delta-\xi)}Bu(\xi)d\xi + \int_{k\delta}^{(k+1)\delta} e^{A[(k+1)\delta-\xi]}Bu(\xi)d\xi. \tag{19}$$

Let $\lambda = k\delta - \xi$, and substituting into (19) gives

$$x(k+1) = e^{A\delta}\underline{x}(k) + e^{A\delta}\int_0^{\delta} e^{A(\delta-\lambda)}Bu(\lambda+k\delta)d\lambda. \tag{20}$$

Replacing $u(\lambda+k\delta)$ by $u(k)$ for all $0 \le \lambda < \delta$, the discrete time system that approximates the continuous time one is then $\underline{x}(k+1) = \bar{A}\underline{x}(k) + \bar{B}u(k)$. Here, $\bar{A} = \sum_{n=0}^{\infty} A^n(\delta)^n/n!$ and $\bar{B} = A^{-1}(\bar{A}-I)^{-1}B$ denote the system matrices.

We assume for convenience that the lumped delay of sensation and perception is the same as the lumped delay of transduction and execution, which is $\tau_s = \tau_a = n_a\delta$. This is not essential; our approach will work even if the delays are different. The dynamics including sensory and activation delay are modeled by introducing a new vector state variable $\underline{z}$ as follows [45]:

$$\underline{z}(k) = [\underline{x}^T(k-n_a), \underline{x}^T(k-n_a+1), \ldots \underline{x}^T(k), \underline{u}^T(k-n_a), \ldots \underline{u}^T(k-1)].$$

Inclusion of the delay in the observations and activation greatly increases the state dimension, thereby changing the optimal control problem substantially. Now the delayed model with noise can be defined in a new state vector $\underline{z}(k)$ as

$$\begin{aligned}\underline{z}(k+1) &= \bar{A}_z\underline{z}(k) + \bar{B}_z\underline{u}(k) + \underline{v}(k)\\ \underline{y}(k) &= \bar{C}_z\underline{z}(k) + \underline{\omega}(k)\end{aligned} \tag{21}$$

where

$$\underline{z}(k) = \begin{bmatrix} z_1(k)\\ z_2(k)\\ z_3(k)\\ \vdots\\ z_{6n_d+4}(k)\end{bmatrix}, \quad \underline{u}(k) = \begin{bmatrix} 0\\ 0\\ \vdots\\ u_1(k)\\ u_2(k)\end{bmatrix}$$

$$\bar{A}_z = \begin{bmatrix} O_{4n_a\times 4} & I_{4n_a\times 4n_a} & O_{4n_a\times 2n_a}\\ O_{4\times 4} & O_{4\times 4(n_a-1)}\ \bar{A}_{4\times 4} & \bar{B}_{4\times 2}\ O_{4\times(2n_a-2)}\\ O_{2n_a\times 4} & O_{2n_a\times 4n_a} & I_{2n_a\times 2n_a}\end{bmatrix}$$

$$\bar{B}_z = \begin{bmatrix} 0 & 0 \\ 0 & 0 \\ \vdots & \vdots \\ 0 & 0 \\ 1 & 0 \\ 0 & 1 \end{bmatrix}, \quad \bar{C}_z = \begin{bmatrix} I_{4\times 4} & \cdots & O \\ \vdots & O_{4n_a\times 4n_a} & \vdots \\ O & \cdots & I_{2n_a\times 2n_a} \end{bmatrix}.$$

The expression for $\underline{y}(k)$ reflects the fact that the original system states are only available to the controller after a delay. The states corresponding to the delayed controls are, in contrast, known to the controller immediately, so these are included in $\underline{y}(k)$. The process noise $\underline{v}(k)$ and measurement noise $\underline{w}(k)$ are both independent WGN with mean zero and covariance Ξ and Θ, respectively, i.e., $\underline{v} \sim N(0, \Xi)$ and $w \sim N(0, \Theta)$. Note that these noise terms model the perturbations as well as any internal random variability in sensing and actuation, including the motor noise [46].

The full state is not available to the controller at every time instant, which complicates the solution because optimal controllers are known to always use full state feedback. The system dynamics is now stochastic and the states and controls exist only in discrete time. Thus the performance measure is revised as

$$J = E\left(\frac{1}{2}\sum_{0}^{\infty}\left[ql_{\text{cop}}^4(\sigma) + r_1u_1^2(k) + r_2u_2^2(k)\right]\right). \quad (22)$$

The discrete-time approximation to the original optimal control problem is to choose the sequence $\underline{u}(k)$ for all integer $k, 0 \leq k < \infty$, so as to minimize (22) subject to the constraints defined in (21).

However, there is one more approximation that is routinely used in engineering applications of MPC to solve this stochastic control problem. The approximation is to impose certainty equivalence, or the separation principle [33]. The idea is to divide the controller into two independent components, a filter/predictor that estimates the current state based on the sensory observations $\underline{y}(\hat{\tau}), 0 \leq \hat{\tau} \leq \tau$ and the control signal $\underline{u}(\hat{\tau}), 0 \leq \hat{\tau} \leq \tau$; and a deterministic feedback controller that uses the mean value of the estimated state vector—we define this to be $\underline{z}(\tau \,|\, \tau)$—as if it were the exact deterministic state vector. For small perturbations, our problem has nearly linear closed-loop dynamics and so the separation of control and estimation should introduce only small deviations from optimality.

The near linearity of the closed-loop dynamics implies that the *Kalman* filter/predictor should be the nearly optimal state estimator for this nonlinear, stochastic, optimal control problem. The controller structure is illustrated in Fig. 3. The use of the *Kalman* filter in movement control has been proposed before. It is inherent in the solution to the LQG-based models. It has also been proposed as a model of sensory integration in posture control [29]. Experimental evidence for the use of such a filter/predictor by the human brain as it performs motor control has been presented [32]. This leaves only the problem of finding an optimal feedback solution to the deterministic control problem. Consider our deterministic problem

$$\text{Minimize} \quad J = \frac{1}{2}\sum_{k=0}^{\infty}\left[ql_{\text{cop}}^4(t) + r_1u_1^2(k) + r_2u_2^2(k)\right]$$

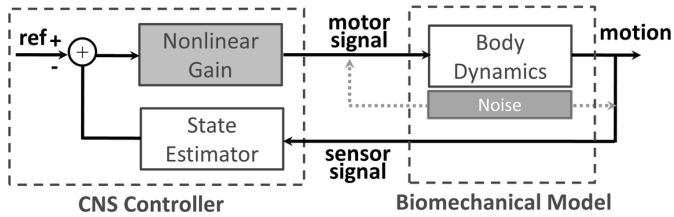

Fig. 3. System diagram of balance control model with delays and noise/perturbations shown. State estimator is assumed to be well approximated by a *Kalman* filter/predictor.

$$\text{Subject to} \quad \underline{z}(k+1) + \bar{A}_z\underline{z}(k) + \bar{B}_z\underline{u}(k)$$
$$\text{and } \underline{z}(0) = \underline{z}_0.$$

We assume the entire initial state vector is available to the controller. This open-loop optimal control problem can be solved for the optimal control, $\underline{u}^{\text{opt}}(\underline{x}_0, k)$, for $k = 0, 1, 2, \ldots, n, \ldots$. We apply the control $\underline{u}^{\text{opt}}(\underline{x}_0, 0)$ as input to the system, which returns the value $\underline{z}(1) = \underline{z}_1$. At $k = 1$ we solve the same open-loop optimal control problem except that the initial condition is $\underline{z}(0) = \underline{z}_1$. The new optimal controller is $\underline{u}^{\text{opt}}(\underline{z}_1, k)$, for $k = 0, 1, 2, \ldots, n, \ldots$ and applying the first control $\underline{u}^{\text{opt}}(\underline{z}_1, 0)$ as input to the actual system generates the value $\underline{z}(2) = \underline{z}_2$. Then we again repeat the previous procedure, i.e., solve the original optimal problem with $\underline{z}(0) = \underline{z}_2$. Continue this indefinitely and the result is the approximately optimal feedback solution to the optimal control problem of (21) and (22). Implementation of the feedback control is generally impossible as it involves solving an infinite horizon optimal control problem instantaneously. In order to solve each open-loop optimal control problem, we apply a second approximation which is to replace the performance measure in (22) with

$$J = \frac{1}{2}\sum_{k=0}^{N^d}\left[ql_{\text{cop}}^4(t) + r_1u_1^2(k) + r_2u_2^2(k)\right].$$

The resulting open-loop optimal control problem now becomes a nonlinear programming problem, which is convex in our case. There are very good methods for solving such problems in a short time [39]. Generally, the approximation involved in replacing ∞ by a reasonably large value for N^d is very minor, as long as N^d is large enough for the closed-loop transients to die down to reasonably near zero. In engineering the initial value used in the real-time optimization is not $\underline{z}_k$ but $\underline{\hat{z}}(k \,|\, k-1)$, the estimate of $\underline{z}_k$ given data up to $k-1$. We apply the *Newton-KKT* method [47], by defining the control vector $\underline{u}(k) = [u_1(k), u_2(k)]$ and a new overall variable $\underline{s} = [\underline{z}(0)^T, \underline{u}(0)^T, \underline{z}(1)^T, \underline{u}(1)^T, \ldots, \underline{u}(N-1)^T, \underline{z}(N)^T]^T$. The constraint imposed by the system dynamics is $A\underline{s} = b$

$$A_s = \begin{bmatrix} I & 0 & \cdots & \cdots & \cdots & O \\ -\bar{A}_z & -\bar{B}_z & I & 0 & \cdots & \vdots \\ \vdots & \vdots & \vdots & \vdots & \vdots & \vdots \\ O & \cdots & -\bar{A}_z & -\bar{B}_z & I & 0 \end{bmatrix}$$

$$b = \begin{bmatrix} \underline{z}(0) \\ O \\ \vdots \\ O \end{bmatrix}.$$

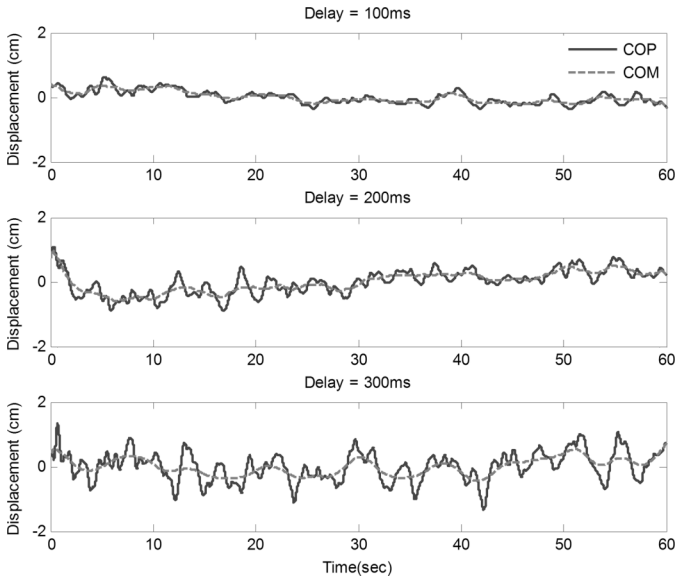

Fig. 4. Trajectories of COP (solid line) with different time delays under fixed perturbation $\|\epsilon\| = 0.01$.

TABLE II
BODY CHARACTERISTICS, DIMENSIONLESS MODEL PARAMETERS AND SIMULATION VARIABLES

M	$76kg$	I_0	$0\,kgm^2$	δ	0.01	$l_{cop}[0]$	$0.18\,cm$
L	$1.76m$	I_1	$0.45\,kgm^2$	N	6000	$u_1[0]$	$0\,Nm$
g	$9.81\,m/s^2$	I_2	$0.35\,kgm^2$	N^d	40	$u_2[0]$	$0\,Nm$

The key step of the method is the repeated solution of the following *Newton-KKT* system of linear equations involving the gradient and the Hessian of $J(\underline{s})$:

$$\begin{bmatrix} \nabla^2 J\left(\underline{s}^{(i)}\right) & A_s^T \\ A_s & O \end{bmatrix} \begin{bmatrix} \Delta \underline{s}_{nt}^{(i)} \\ \underline{w} \end{bmatrix} = \begin{bmatrix} -\nabla J\left(\underline{s}^{(i)}\right) \\ O \end{bmatrix}.$$

Here $\Delta \underline{s}_{nt}^{(i)}$ is the *Newton* step at the ith iteration. To solve more efficiently, we used the *Schur* Complement to reduce the system to $\nabla^2 J(\underline{s}^{(i)}) \Delta \underline{s}_{nt}^{(i)} + A_s^T w = -\nabla J(\underline{s}^{(i)})$.

V. RESULTS

We have successfully solved the constrained nonlinear optimal control problem using the method described previously. In this section, we show that the optimal feedback solution replicates two of the important experimentally observed features of postural control. The parameters and coefficients in the simulations are based on the dynamic model defined in (21) using body parameters from Peterka [30] as shown in Table II. The MPC method was used to compute the approximately optimal feedback control, with a look-ahead time of 4 s and a sampling interval of 0.1 s, resulting in a predictive horizon $N^d = 40$. The dimensionless results are converted back to real units for comparison with the experimental measurements.

A. Small Perturbations

We first consider the steady-state response of the closed-loop system to small perturbations—white Gaussian noise with a standard deviation of 0.01. This noise level models the case where only neuronal noise acts on the system; the posture is otherwise unperturbed. The system starts at an initial position in which its COP is set to its equilibrium value, i.e., $l_{\rm cop}[0] = 0.18$ cm. We use q as the weight on the COP deviation. The parameters r_1 and r_2 are the weights on the control torques at the ankle and hip joints, respectively.

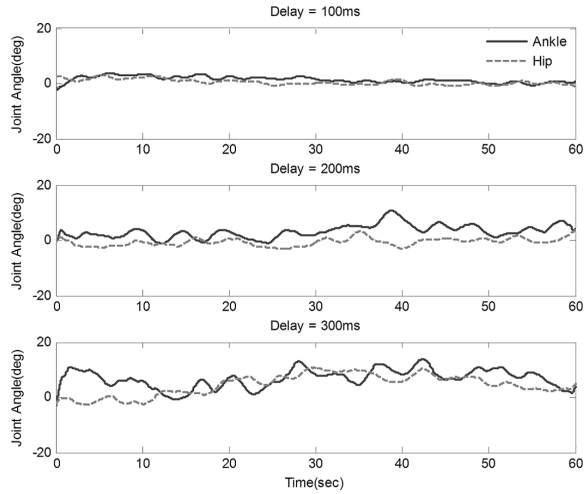

Fig. 5. Joint angle trajectories of ankle joint (solid line) and hip joint (dotted line) with different time delays under fixed perturbation $\|\epsilon\| = 0.01$.

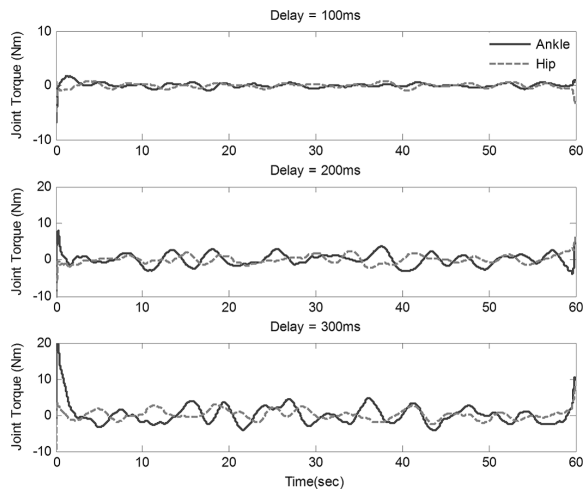

Fig. 6. Ankle (solid line) and hip (dotted line) torques with different time delay under fixed perturbation $\|\epsilon\| = 0.01$.

To understand the effect of the choice of q, r_1 and r_2 on the solution, note first that we have chosen $q = 10$ and $r_1 = r_2 = 1$, thereby weighting the two controllers equally. The relationship $q l_{\rm cop}^4(k) = [l_{\rm cop}(k)/(1/q)^{1/4}]^4$ shows that this choice for q underweights deviations of the COP that are less than 0.56. Changing q would change the value of $l_{\rm cop}$ at which this transition occurs. Three different values of delay were applied in this set of simulations: 100, 200, and 300 ms.

The resulting motion of the COP is plotted in Fig. 4. The trajectories of the ankle and hip angles for WGN of standard deviation 0.01 and three different delays (100, 200, and 300 ms) are depicted in Fig. 5. The corresponding control torques are shown in Fig. 6. The ankle angle appears to undergo greater

TABLE III
SWAY NORM AND CONTROL ENERGY WITH 100 MS DELAY. NORMS ARE: $\|\phi\|_1 = \sum_{k=1}^{N} |\phi_k|, \|\phi\|_2 = \sum_{k=1}^{N} |\phi_k|^2, \|\phi\|_\infty = \max_{0\le k\le N}, |\phi_k|$

Noise Level	$\|\epsilon\| = 0.01$								
Ankle Joint	$\frac{1}{N}\|\phi_*\|_1$	$\frac{1}{N}\|\phi_*\|_2$	$\|\phi_*\|_\infty$	$\sum \|u\Delta\dot{\phi}\|$	Hip Joint	$\frac{1}{N}\|\phi_*\|_1$	$\frac{1}{N}\|\phi_*\|_2$	$\|\phi_*\|_\infty$	$\sum \|u\Delta\dot{\phi}\|$
NQR	2.1199	0.0344	4.6295	0.1387	NQR	1.4037	0.0229	4.5665	0.0696
LQR	2.0684	0.0286	3.9076	0.3593	LQR	0.9683	0.0172	3.5982	0.1907
Noise Level	$\|\epsilon\| = 0.1$								
Ankle Joint	$\frac{1}{N}\|\phi_*\|_1$	$\frac{1}{N}\|\phi_*\|_2$	$\|\phi_*\|_\infty$	$\sum \|u\Delta\dot{\phi}\|$	Hip Joint	$\frac{1}{N}\|\phi_*\|_1$	$\frac{1}{N}\|\phi_*\|_2$	$\|\phi_*\|_\infty$	$\sum \|u\Delta\dot{\phi}\|$
NQR	3.9821	0.0630	9.7918	0.2306	NQR	4.9274	0.0688	8.4569	0.8044
LQR	2.9908	0.0458	5.0391	3.5747	LQR	2.6929	0.0401	5.9931	1.6208
Noise Level	$\|\epsilon\| = 0.5$								
Ankle Joint	$\frac{1}{N}\|\phi_*\|_1$	$\frac{1}{N}\|\phi_*\|_2$	$\|\phi_*\|_\infty$	$\sum \|u\Delta\dot{\phi}\|$	Hip Joint	$\sum \|u\Delta\dot{\phi}\|$	$\frac{1}{N}\|\phi_*\|_2$	$\|\phi_*\|_\infty$	$\sum \|u\Delta\dot{\phi}\|$
NQR	4.5493	0.0688	10.3877	1.1041	NQR	9.5799	0.1432	11.3503	2.425
LQR	3.9821	0.0630	10.1757	10.1377	LQR	3.2200	0.0516	10.3591	12.0985

TABLE IV
SWAY NORM AND CONTROL ENERGY WITH 200 MS DELAY. SWAY NORM UNIT: DEGREE; ENERGY UNIT: KG $(\mathrm{m/s})^2$

Noise Level	$\|\epsilon\| = 0.01$								
Ankle Joint	$\frac{1}{N}\|\phi_*\|_1$	$\frac{1}{N}\|\phi_*\|_2$	$\|\phi_*\|_\infty$	$\sum \|u\Delta\dot{\phi}\|$	Hip Joint	$\frac{1}{N}\|\phi_*\|_1$	$\frac{1}{N}\|\phi_*\|_2$	$\|\phi_*\|_\infty$	$\sum \|u\Delta\dot{\phi}\|$
NQR	5.0535	0.0745	8.2076	1.1767	NQR	3.6841	0.0516	6.1306	0.4519
LQR	3.3747	0.0573	8.1589	2.8265	LQR	2.0168	0.0286	4.3602	1.5766
Noise Level	$\|\epsilon\| = 0.1$								
Ankle	$\frac{1}{N}\|\phi_*\|_1$	$\frac{1}{N}\|\phi_*\|_2$	$\|\phi_*\|_\infty$	$\sum \|u\Delta\dot{\phi}\|$	Hip Joint	$\frac{1}{N}\|\phi_*\|_1$	$\frac{1}{N}\|\phi_*\|_2$	$\|\phi_*\|_\infty$	$\sum \|u\Delta\dot{\phi}\|$
NQR	5.5691	0.1203	19.6009	3.7584	NQR	7.0417	0.1604	21.5661	2.4519
LQR	3.5638	0.0917	15.8079	4.9491	LQR	3.1427	0.0688	12.6738	3.5045
Noise Level	$\|\epsilon\| = 0.5$								
Ankle Joint	$\frac{1}{N}\|\phi_*\|_1$	$\frac{1}{N}\|\phi_*\|_2$	$\|\phi_*\|_\infty$	$\sum \|u\Delta\dot{\phi}\|$	Hip Joint	$\frac{1}{N}\|\phi_*\|_1$	$\frac{1}{N}\|\phi_*\|_2$	$\|\phi_*\|_\infty$	$\sum \|u\Delta\dot{\phi}\|$
NQR	8.5600	0.2063	25.8576	5.5766	NQR	9.5799	0.2693	27.8114	4.3737
LQR	4.7326	0.1547	16.9137	16.2654	LQR	3.2200	0.1089	14.7995w	12.3162

excursions than the hip angle. To quantify this we then compute three different norms of the respective trajectories for the two joints: $\|\phi\|_1 = \sum_{k=1}^{N} |\phi_k|$, $\|\phi\|_2 = \sum_{k=1}^{N} |\phi_k|^2$, and $\|\phi\|_\infty = \max_{0\le k\le N} |\phi_k|$.

The results for delays of both 100 and 200 ms are shown in Tables III and IV. Notice that no matter what norm is used, the ankle joint angle always has greater movement than the hip joint. For comparison, we computed the controls and simulated the closed-loop system for an LQR controller based on the same parameters as our NQR controller. The only difference in the problems is that l_{cop} is weighted quadratically in the performance measure instead of quartically. The resulting feedback controls are different but for these small perturbations the optimal LQR also gives larger movement of the ankle than of the hip angle.

B. Large Perturbations

In this simulation of the steady state response, all the parameters were kept the same as before except for a larger perturbation—WGN with a standard deviation of 0.1. In Fig. 7, the ankle and hip joint trajectories are plotted for the three different delays and the larger noise level. It is visually obvious that the hip angular motion is larger than that of the ankle angle.

Table III gives the quantitative results in terms of the respective norms, confirming the visual impression. The hip angular motion is larger than that of the ankle when the noise level is $\|\epsilon\| = 0.1$ or $\|\epsilon\| = 0.5$. In this case, the LQR controller gives ankle angle motion that is larger than that of the hip angle for all

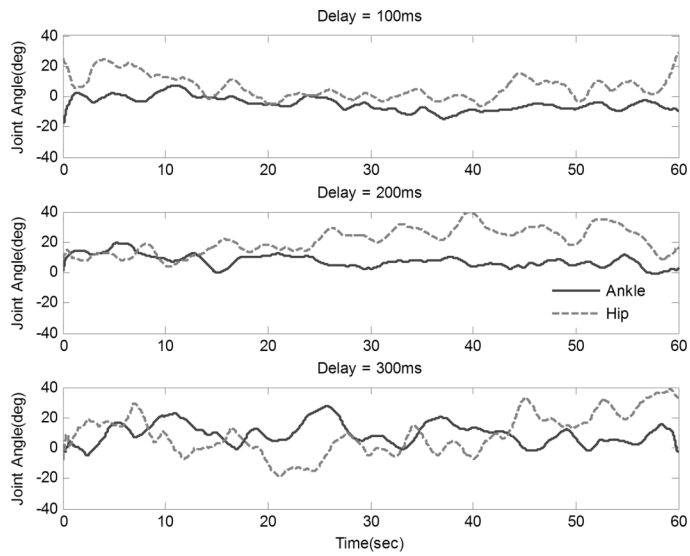

Fig. 7. Joint angle trajectories of ankle (solid line) and hip joint (dotted line) with different time delays under fixed perturbation $\|\epsilon\| = 0.1$.

choices of noise level and delay. This is not only different from the NQR, it is also different from the experimental observations.

VI. DISCUSSION

Collins and DeLuca proposed an analysis technique called the stabilogram diffusion function (SDF) [8] to better understand the postural sway. The SDF measures the similarity of

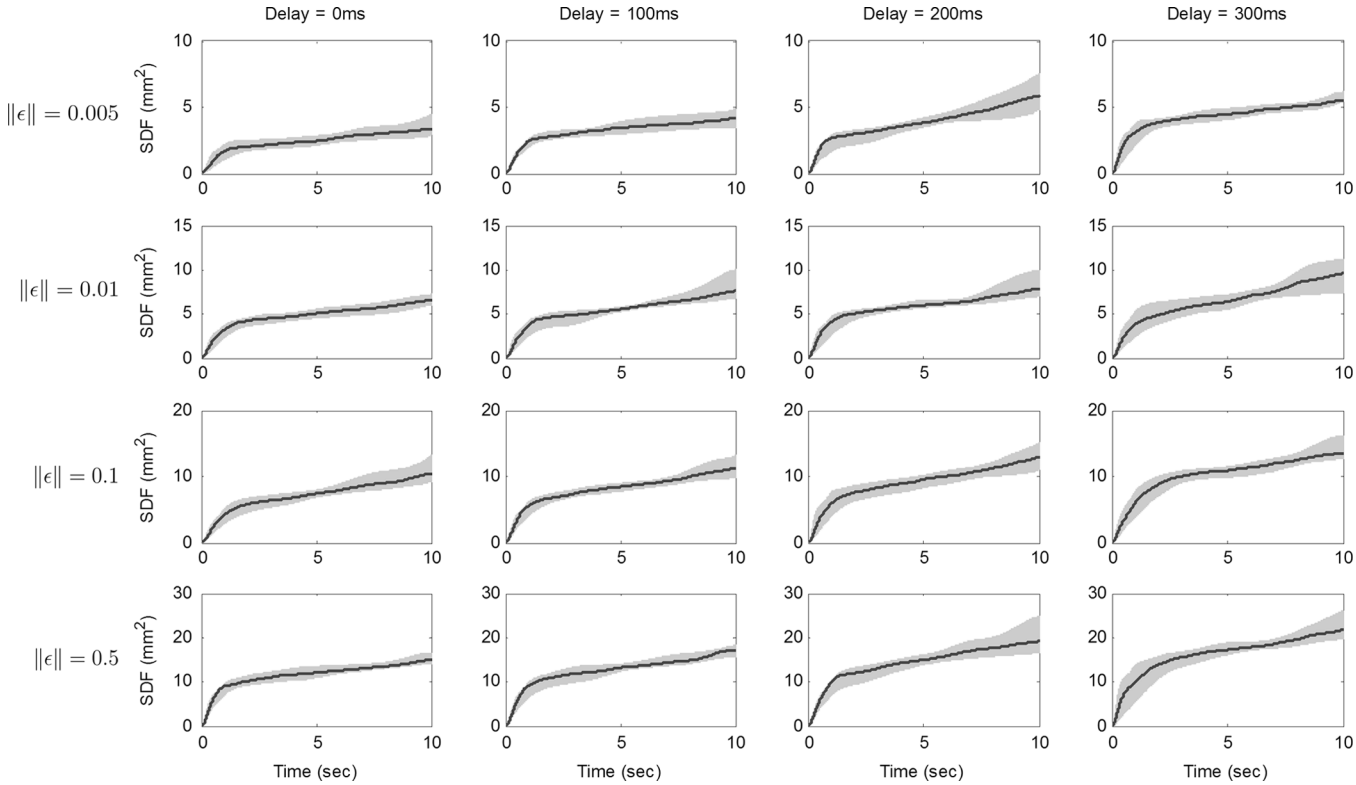

Fig. 8. SDF with different delays driven by WGN with different standard deviations starting from the equilibrium point of COP. First column has zero delay, second column has delay of 100 ms, third has a 200-ms delay, and fourth has a 300-ms delay. Row one has perturbation $\|\epsilon\| = 0.005$, row two has perturbation $\|\epsilon\| = 0.01$, row three has perturbation $\|\epsilon\| = 0.1$, and row four has perturbation $\|\epsilon\| = 0.5$. Parameters for this subject are: height $= 1.76$ m and weight $= 70$ kg. Weight for COP in the performance measure was $q = 10$. In order to test the robustness of the control, we used ten different WGN generators for each value of standard deviation. Gray shading indicates region occupied by multiple simulations.

the average COP between different time intervals and describes the relationship between the time interval of motion and the average of corresponding changes in position. The SDF for the COP is defined as: $\langle \Delta l_{\text{cop}}^2 \rangle = \langle [l_{\text{cop}}(t+\Delta t) - l_{\text{cop}}(t)]^2 \rangle$ where $\langle \cdot \rangle$ denotes the ensemble mean of the time series. SDF is very sensitive to sway amplitude and velocity. At $\Delta t = 0$, $\langle \Delta l_{\text{cop}}^2 \rangle$ is zero. As Δt increases, $\langle \Delta l_{\text{cop}}^2 \rangle$ will increase because $l_{\text{cop}}(t)$ and its time shifted value, $l_{\text{cop}}(t + \Delta t)$, become less similar to each other. In our simulation, the Δt ranges from 0 to 10 s.

Peterka applied a PID controller with different feedback delays and a single joint model to replicate the two-part form of SDF observed experimentally [30]. For our MPC-based model, Figs. 8 and 9 show the results of an investigation of the SDF resulting from different choices for the delay and noise level.

In Fig. 8, all of the choices give the characteristic shape of the experimentally observed SDF. Careful examination of the figure shows that the initial rise of the SDF partially depends on the delay—longer delays decrease the slope and increase the height of the corner.

Fig. 9 shows that the simulated SDF can be matched closely to the experimental one by appropriate choice of weight on the COP deviations and the delay. It is, in fact, quite likely that the experimental SDF does depend on the delays in the subject's responses. The 125-ms delay that best matches the experimental delay is consistent with only proprioceptive delays without vision.

To further investigate the control strategy and the coordination process, we estimated the energy consumed at each joint, which is computed as $E_i = \sum_{k=0}^{N} |u_i(k)\Delta\dot{\phi}_i(k)|$. E_1 gives

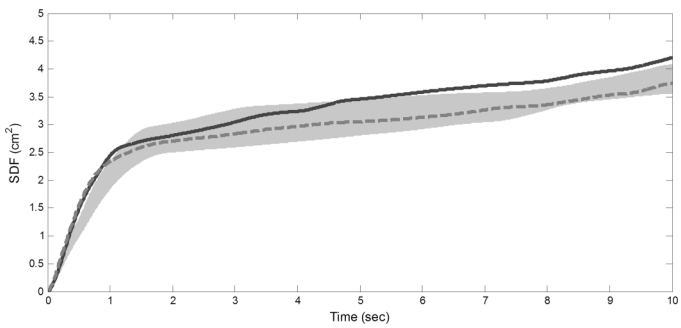

Fig. 9. Simulated SDF (dashed line) compared with experimental SDF (solid line). Dashed line is mean of ten different simulated SDFs, light shading shows range of ten different noise seeds with same standard deviation, $\|\epsilon\| = 0.005$. To best approximate experimental results, penalty for deviations from zero of COP was chosen to be $q = 15$, and delay was 125 ms. Shading shows boundary of simulation results with different noise seeds.

the energy consumed by the ankle torque generator, E_2 gives the value for the hip torque generator. We make the assumption that energy is expended regardless of the sign of the product of angular velocity and torque. This ignores some amount of energy storage in tendons and muscle, which is likely to be small given the small excursions and the low torques that are involved. The results are shown in Tables III and IV. Notice that the energy expended is substantially less than that needed by the directly comparable *LQR* controller. Control engineers know that a small dead zone near the desired equilibrium point can save energy as well as wear and tear on the actuator.

This may, in fact, provide a functional explanation for the experimentally observed sensory dead zones. In order to confirm this, the ideal torque generators should be replaced by more realistic muscle models that include the effects of kinematics on force generation and energy consumption [50] as well as an accurate representation of the nonlinear series elasticity of the tendon [57]; such models are incorporated into Musculoskeletal Modeling Software [58].[1]

Although the control mechanism proposed here is a natural one for the human, we certainly do not claim that the human implements the controller in the way that we have. A large collection of neurons that provide the input signal to the muscles are threshold devices. They can implement any nonlinear gain by just changing their thresholds. In fact, the size principle [48] suggests that the gain of any feedback controller using muscle as the actuator should increase faster than linearly as perturbation amplitude increases. Thus, our nonlinear feedback controller is as easy, if not easier, for the human central nervous system to implement than any linear one. With regard to the predictor, we do not insist on the *Kalman* filter/predictor, because any good predictor can be expected to work reasonably well as an alternative. It is clear that humans use prediction in their motor control system. For example, running humans predict the time and force of the impact as each foot hits the ground [49] and further evidence has been presented in [32].

Finally, the proposed model and the approach used to solve for the feedback optimal control can be elaborated in numerous ways. The quartic performance criterion could be replaced with higher power functions as long as they are even numbers. It could also be extended to many other control applications where energy expenditure and/or actuator wear and tear are important.

VII. Conclusion

We have proposed an optimal control model for the regulation of upright posture in the sagittal plane. A double inverted pendulum that is used to approximate the human is controlled by joint torques at the ankle and hip. The neural delays from sensation, perception, transduction and execution were incorporated into the neuromusculoskeletal dynamics. The proposed optimization criterion is quadratic in the control effort but quartic in the COP, which is a good measurement for assessing the stability of quiet standing. This objective function provides a tradeoff between the allowed deviations of the COP from its nominal value and the amount of control required to correct for these deviations. By utilizing the MPC technique, which gives a good approximation to the optimal feedback control, we provide a numerical solution to the analytically unsolvable nonlinear optimal control problem.

The simulation results of the optimal feedback control show that the proposed model of posture regulation replicates two of the experimentally observed attributes of the human's controller. First, the responses to different amplitudes of perturbation are qualitatively and quantitatively different. Small perturbations result in primarily ankle motion while larger perturbations produce more hip motion than ankle motion. Second, the model replicates the characteristics of the experimentally observed SDF. The simulation has also demonstrated that the proposed model results in a control strategy that should consume relatively less energy than linear feedback control. Although this has not yet been observed experimentally, it is certainly plausible that using less energy is a goal of the human postural regulation system.

[1]Available at http://mddf.usc.edu.

Acknowledgment

The healthy human subject data were collected on AMTI's AccuSway^{PLUS} Balance Platform (Watertown, MA) and preprocessed by AMTI *Balance Clinic Program*. All experiments were performed at the clinics of the Rehabilitation Department, West China School of Medicine, Sichuan University, P. R. China. The authors would like to express special thanks to Ms. Y. Yang for experiment assistance and Dr. C. He for the valuable discussions.

References

[1] F. B. Horak and J. M. Macpherson, "Postural orientation and equilibrium," in *Handbook of Physiology. Exercise: Regulation and Integration of Multiple Systems. Control of Respiratory and Cardiovascular Systems*. New York: Oxford Univ. Press, 1996, pp. 255–292.

[2] N. Accornero *et al.*, "Clinical multisegmental posturography: Age-related changes in stance control," *Electroencephalogr. Clin. Neurophysiol./Electromyogr. Motor Control*, vol. 105, no. 3, pp. 213–219, 1997.

[3] V. P. Panzer *et al.*, "Biomechanical assessment of quiet standing and changes associated with aging," *Arch. Phys. Medicine Rehab.*, vol. 76, pp. 151–157, 1995.

[4] R. Fitzpatrick and D. I. McCloskey, "Proprioceptive, visual and vestibular thresholds for the perception of sway during standing in humans," *J. Physiol.*, vol. 478, pp. 173–186, 1994.

[5] R. C. Fitzpatrick *et al.*, "Ankle stiffness of standing humans in response to imperceptible perturbation: Reflex and task-dependent components," *J. Physiol.*, vol. 454, pp. 533–547, 1992.

[6] J. J. Jeka *et al.*, "Coupling of fingertip somatosensory information to head and body sway," *Exp. Brain Res.*, vol. 113, pp. 475–483, 1997.

[7] K. H. Mauritz and V. Dietz, "Characteristics of postural instability induced by ischemic blocking of leg afferents," *Exp. Brain Res.*, vol. 38, pp. 117–119, 1980.

[8] J. J. Collins and C. J. Luca, "The effects of visual input on open-loop and closed-loop postural control mechanisms," *Exp. Brain Res.*, vol. 103, pp. 151–163, 1995.

[9] T. Dijkstra *et al.*, "Frequency dependence of the action-perception cycle for postural control in a moving visual environment: Relative phase dynamics," *Biol. Cybern.*, vol. 71, pp. 489–501, 1994.

[10] B. L. Day *et al.*, "Human body-segment tilts induced by galvanic stimulation: A vestibularly driven balance protection mechanism," *J. Physiol.*, vol. 500, pp. 661–672, 1997.

[11] M. Lacour *et al.*, "Sensory strategies in human postural control before and after unilateral vestibular neurotomy," *Exp. Brain Res.*, vol. 115, pp. 300–310, 1997.

[12] D. A. Winter *et al.*, "Stiffness control of balance in quiet standing," *J. Neurophysiol.*, vol. 80, pp. 1211–1221, 1998.

[13] F. Bell, *Principles of Mechanics and Biomechanics*. Cheltenham, U.K.: Stanley Thornes, 1998.

[14] R. Fitzpatrick *et al.*, "Loop gain of reflexes controlling human standing measured with the use of postural and vestibular disturbances," *J. Neurophysiol.*, vol. 76, pp. 3994–4008, 1996.

[15] J. J. Collins and C. J. De Luca, "Random walking during quiet standing," *Phys. Rev. Lett.*, vol. 73, p. 764, 1994.

[16] D. A. Winter *et al.*, "Ankle muscle stiffness in the control of balance during quiet standing," *J. Neurophysiol.*, vol. 85, pp. 2630–2633, 2001.

[17] J. J. Collins and C. J. Luca, "Open-loop and closed-loop control of posture: A random-walk analysis of center-of-pressure trajectories," *Exp. Brain Res.*, vol. 95, pp. 308–318, 1993.

[18] Y. Aramaki *et al.*, "Reciprocal angular acceleration of the ankle and hip joints during quiet standing in humans," *Exp. Brain Res.*, vol. 136, pp. 463–473, 2001.

[19] R. Fitzpatrick *et al.*, "Stable human standing with lower-limb muscle afferents providing the only sensory input," *J. Physiol.*, vol. 480.2, pp. 395–403, 1994.

[20] J. Jeka *et al.*, "Multisensory information for human postural control: Integrating touch and vision," *Exp. Brain Res.*, vol. 134, pp. 107–125, 2000.

[21] J. J. Jeka *et al.*, "The structure of somatosensory information for human postural control," *Motor Contr.*, vol. 2, pp. 13–33, 1998.

[22] A. D. Kuo, "An optimal control model for analyzing human postural balance," *IEEE Trans. Biomed. Eng.*, vol. 42, no. 1, pp. 87–101, Jan. 1995.

[23] J. He *et al.*, "Feedback gains for correcting small perturbations to standing posture," *IEEE Trans. Automat. Control*, vol. 36, no. 2, pp. 322–332, Feb. 1991.
[24] E. F. Camacho and C. Bordons, *Model Predictive Control*, 2nd ed. New York: Springer, 2004.
[25] J. B. Rawlings, "Tutorial overview of model predictive control," *IEEE Trans. Contr. Syst.*, vol. 20, no. 1, pp. 38–52, Feb. 2000.
[26] S. J. Qin and T. A. Badgwell, "A survey of industrial model predictive control technology," *Contr. Eng. Practice*, vol. 11, pp. 733–764, 2003.
[27] L. M. Nashner, "Adapting reflexes controlling the human posture," *Exp. Brain Res.*, vol. 26, pp. 59–72, 1976.
[28] L. M. Nashner, "Fixed patterns of rapid postural responses among leg muscles during stance," *Exp. Brain Res.*, vol. 30, pp. 13–24, 1977.
[29] H. van der Kooij *et al.*, "A multisensory integration model of human stance control," *Biol. Cybern.*, vol. 80, pp. 299–308, 1999.
[30] R. J. Peterka, "Postural control model interpretation of stabilogram diffusion analysis," *Biol. Cybern.*, vol. 82, pp. 335–343, 2000.
[31] E. Todorov and M. I. Jordan, "Optimal feedback control as a theory of motor coordination," *Nature Neurosci.*, vol. 5, pp. 1226–1235, 2002.
[32] R. Shadmehr and J. W. Krakauer, "A computational neuroanatomy for motor control," *Exp. Brain Res.*, vol. 185, pp. 359–381, 2008.
[33] M. Athans and P. L. Falb, *Optimal Control*. New York: McGraw–Hill, 1966.
[34] R. Johansson *et al.*, "Optimal coordination and control of posture and movements," *J. Physiol.-Paris*, vol. 103, pp. 159–177.
[35] W. S. Levine, *The Control Handbook*, 1st ed. Boca Raton, FL: CRC Press, 1996.
[36] P. G. Morasso and M. Schieppati, "Can muscle stiffness alone stabilize upright standing?," *J. Neurophysiol.*, vol. 82, pp. 1622–1626, 1999.
[37] R. J. Peterka and M. S. Benolken, "Relation between perception of vertical axis rotation and vestibulo-ocular reflex symmetry," *J. Vestib. Res.*, vol. 2, pp. 59–69, 1992.
[38] D. A. Winter, *Biomechanics and Motor Control*, 3rd ed. Hoboken, NJ: Wiley, 2004.
[39] J. Milton, "The time-delayed inverted pendulum: Implications for human balance control," *Chaos*, vol. 19, p. 026110, 2009.
[40] R. J. Peterka, "Sensorimotor integration in human postural control," *J. Neurophysiol.*, vol. 88, pp. 1097–1118, 2002.
[41] R. Nijhawan, "Visual prediction: Psychophysics and neurophysiology of compensation for time delays," *Behavioral Brain Sci.*, vol. 31, pp. 179–198, 2008.
[42] R. S. Woodworth and H. Schlosberg, *Experimental Psychology*. New York: Holt Rinehart Winston, 1954.
[43] Y. Li and W. S. Levine, "An optimal control model for human postural regulation," in *Proc. 2009 Am. Control Conf.*, 2009, pp. 1143–1148.
[44] Y. Li and W. S. Levine, "An optimal model predictive control model for human postural regulation," presented at the *17th Mediterranean Conf. Control Automation*, Greece, 2009.
[45] Y. Li and W. S. Levine, "Models for human postural regulation that include realistic delays and partial observations," in *Proc. 48th IEEE Conf. Decision Control Conf.*, Shanghai, China, 2009, pp. 4590–4595.
[46] K. E. Jones *et al.*, "Sources of signal-dependent noise during isometric force production," *J. Neurophysiol.*, vol. 88, pp. 1533–1544, 2002.
[47] S. P. Boyd and L. Vandenberghe, *Convex Optimization*. Cambridge, U.K.: Cambridge Univ. Press, 2004.
[48] G. E. Loeb and C. Ghez, , E. R. Kandel, Ed. *et al.*, "The motor unit and motor action," in *Principles Neural Sci.*, 4th ed. New York: McGraw-Hill, 2000, pp. 676–686.
[49] N. Bernstein, *The Coordination and Regulation of Movement*. New York: Pergamon, 1967.
[50] C. M. Harris and D. M. Wolpert, "Signal dependent noise determines motor planning," *Nature*, vol. 394, no. 6695, pp. 780–784, 1998.
[51] F. C. Anderson and M. G. Pandy, "Static and dynamic optimization solutions for gait are practically equivalent," *J. Biomech.*, vol. 34, pp. 153–161, 2001.
[52] M. G. Pandy, F. E. Zajac, E. Sim, and W. S. Levine, "An optimal control model for maximum-height jumping," *J. Biomech.*, vol. 23, pp. 1185–1198, 1990.
[53] C. C. Raasch, F. E. Zajac, B. Ma, and W. S. Levine, "Muscle coordination of maximum speed pedaling," *J. Biomech.*, vol. 30, pp. 595–602, 1997.
[54] P. V. Komi, M. Salonen, M. Jarvinen, and O. Kokko, "In vivo registration of Achilles tendon forces in man I. Methodological development," *Int. J. Sports Med.*, 1987.
[55] W. E. Byerly, *An Introduction to the Use of Generalized Coordinates in Mechanics and Physics*. New York: Dover, 1965.
[56] C. Nicol and P. V. Komi, "Significance of passively induced stretch reflexes on achilles tendon force enhancement," *Muscle Nerve*, vol. 21, no. 11, pp. 1546–1548, 1998.
[57] S. H. Scott and G. E. Loeb, "The mechanical properties of the aponeurosis and tendon of the cat soleus muscle during whole-muscle isometric contractions," *J. Morph.*, vol. 224, pp. 73–86, 1995.
[58] R. Davoodi, C. Urata, M. Hauschild, M. Khachani, and G. E. Loeb, "Model-based development of neural prostheses for movement," *IEEE Trans. Biomed. Eng.*, vol. 54, no. 11, pp. 1909–1918, Nov. 2007.

Yao Li received the B.S. degree in electrical engineering from Sichuan University, Chengdu, China, in 2002, and the Ph.D. degree in electrical and computer engineering, from the University of Maryland, College Park, in 2010.

Since then, he has been working as a Research Associate at the University of Southern California, Los Angeles. He is mainly interested in the application of control theory and modeling of complex systems to the understanding and treatment of human sensorimotor disorders. He was a Visiting Scholar at the National Center for Simulation in Rehabilitation Research (NCSRR), Stanford University, in 2011. He is interested in developing the optimal estimation algorithms for deriving command signals for prosthetic limbs from the residual peripheral nervous system of amputees. He is also interested in the development and experimental validation of models of sensorimotor learning that have important clinical implications and robotic applications of a robust tactile sensor array that mimics the mechanical properties and distributed touch receptors of the human fingertip.

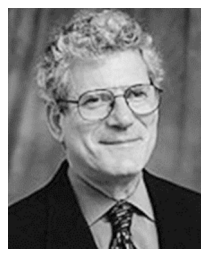

William S. Levine (F'02) received the B.S., M.S., and Ph.D. degrees from Massachusetts Institute of Technology, Cambridge.

He is a Research Professor of electrical and computer engineering at the University of Maryland, College Park. He is the coauthor of *Using MATLAB to Analyze and Design Control Systems* (Benjamin/Cummings, 1992, 2nd Ed., 1995). He is the editor of *The Control Handbook* (CRC Press in cooperation with IEEE Press, 1996, 2nd Ed., 2011). He is the coeditor of *The Handbook of Networked and Embedded Control Systems* (Birkhauser, 2005). He is also the Editor for Birkhauser's *Control Engineering Series*.

Dr. Levine is a member of SIAM, a Distinguished Member of the IEEE Control Systems Society, and has been President of the IEEE Control Systems Society. He is a recipient of the IEEE's Third Millennium Medal. *The Control Handbook* was named best engineering handbook published in 1996 by the Association of American Publishers.

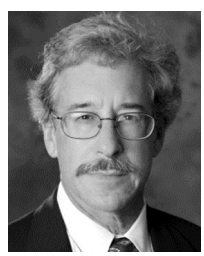

Gerald E. Loeb (M'98) received the B.A. and M.D. degrees from Johns Hopkins University, Baltimore, MD, in 1969 and 1972, respectively, and did one year of surgical residency at the University of Arizona.

He joined the Laboratory of Neural Control at the National Institutes of Health from 1973 to 1988. He was a Professor of physiology and biomedical engineering at Queen's University in Kingston, Canada, from 1988 to 1999, and is now a Professor of biomedical engineering and Director of the Medical Device Development Facility, University of Southern California, Los Angeles. He was one of the original developers of the cochlear implant to restore hearing to the deaf and was Chief Scientist for Advanced Bionics Corporation from 1994 to 1999, manufacturers of the Clarion cochlear implant. He is holder of 52 issued U.S. patents and author of over 200 scientific papers.

Dr. Loeb is a Fellow of the American Institute of Medical and Biological Engineers.